



Communication

Suitability of Low-Cost Sensors for Submicron Aerosol Particle Measurement

Daniel Stoll * , Maximilian Kerner, Simon Paas and Sergiy Antonyuk 

Institute of Particle Process Engineering, University of Kaiserslautern-Landau, 67663 Kaiserslautern, Germany; maximilian.kerner@mv.uni-kl.de (M.K.); simon.paas@mv.rptu.de (S.P.); sergiy.antonyuk@mv.rptu.de (S.A.)

* Correspondence: daniel.stoll@mv.rptu.de

Abstract: The measurement and assessment of indoor air quality in terms of respirable particulate constituents is relevant, especially in light of the COVID-19 pandemic and associated infection events. To analyze indoor infectious potential and to develop customized hygiene concepts, the measurement monitoring of the anthropogenic aerosol spreading is necessary. For indoor aerosol measurements usually standard lab equipment is used. However, these devices are time-consuming, expensive and unwieldy. The idea is to replace this standard laboratory equipment with low-cost sensors widely used for monitoring fine dust (particulate matter—PM). Due to the low acquisition costs, many sensors can be used to determine the aerosol load, even in large rooms. Thus, the aim of this work is to verify the measurement capability of low-cost sensors. For this purpose, two different models of low-cost sensors are compared with established laboratory measuring instruments. The study was performed with artificially prepared NaCl aerosols with a well-defined size and morphology. In addition, the influence of the relative humidity, which can vary significantly indoors, on the measurement capability of the low-cost sensors is investigated. For this purpose, a heating stage was developed and tested. The results show a discrepancy in measurement capability between low-cost sensors and laboratory measuring instruments. This difference can be attributed to the partially different measuring method, as well as the different measuring particle size ranges. The determined measurement accuracy is nevertheless good, considering the compactness and the acquisition price of the low-cost sensors.



Citation: Stoll, D.; Kerner, M.; Paas, S.; Antonyuk, S. Suitability of Low-Cost Sensors for Submicron Aerosol Particle Measurement. *Appl. Syst. Innov.* **2023**, *6*, 69. <https://doi.org/10.3390/asi6040069>

Academic Editor: Subhas Mukhopadhyay

Received: 30 June 2023

Revised: 1 August 2023

Accepted: 4 August 2023

Published: 8 August 2023



Copyright: © 2023 by the authors. Licensee MDPI, Basel, Switzerland. This article is an open access article distributed under the terms and conditions of the Creative Commons Attribution (CC BY) license (<https://creativecommons.org/licenses/by/4.0/>).

Keywords: monitoring; low-cost sensors; dynamic change process; humidity influence on particulate matter size

1. Introduction

Given the COVID-19 pandemic and related infection outbreaks, measuring and assessing indoor air quality in terms of respirable particle constituents are important. Viruses, such as coronavirus SARS-CoV-2, can enter the indoor air environment via liquid droplets exhaled by an infected person during coughing, sneezing or talking [1–3]. The longer the residence time and concentration of the particles in the air, the greater the probability that another person in this room will inhale them [4]. The local particle concentration and residence time of the exhaled aerosol change while spreading in the indoor air environment. When exhaled, droplets with a size distribution in the micron range are formed and released into the air environment. The larger droplets have a higher sedimentation velocity and settle quickly, while the smaller droplets can stay in the air longer and can also spread out over a greater distance [5,6]. The evaporation leads to a reduction in the particle size, which is related to an increased residence time [7,8]. The inhaled particles are mostly dried solid components of droplets in the submicron size range [9,10]. Consequently, exhaled and inhaled aerosols have different properties regarding particle size distribution, local concentration and moisture content.

To analyze the indoor infectious potential and to develop customized hygiene concepts, the detection of the anthropogenic aerosol spreading in public buildings (schools,

hospitals, etc.) is necessary. For indoor aerosol measurements, standard laboratory equipment (Scanning Mobility Particle Sizer, Electrical Aerosol Analyzer, etc.) is used [11–14]. However, these devices are time-consuming, expensive and unwieldy. Moreover, many measurement devices are needed to characterize the spread of aerosols in large rooms in detail [15–20].

The idea is to realize the monitoring of anthropogenic submicron aerosols with the help of low-cost sensors, which are usually used for the measurements of airborne particulate matter. It has already been shown that a network of multiple low-cost sensors can be used to detect indoor smoke exposure from wildfire [21], formaldehyde, carbon dioxide and total volatile organic compounds [22], as well as general indoor air quality [23–26]. The improvement of air quality in many urban areas during the pandemic lockdown was also confirmed by measurements with low-cost sensors [27,28]. In addition, a system of various low-cost environmental sensors that monitored factors such as temperature, humidity, CO₂, the number of people and the dynamics of speech was used to study the spread of COVID-19 in a space [29]. Although many studies demonstrated the effectiveness of low-cost sensors when applied for PM monitoring, it remains open to interpretation how they are calibrated in the first place and how their measurement accuracy is under realistic conditions. In addition, it would be essential to demonstrate the stability of the initial calibration data in terms of time [30–32]. The influence of air humidity on different aerosol measurement devices, which results in a too-high and therefore false particle detection, has already been investigated in several works [33–37].

A conceptual approach for indoor air monitoring is developed in which standard devices are replaced by low-cost sensors and fine-dust analysis (PM) is used as a central evaluation factor, with PM_{2.5} values as the measured variables. Applying this concept to anthropogenic droplet aerosols raises the question of how reliable the low-cost sensors are for the measurement of submicron particles. On the other hand, how suitable are they for handling the influence of high air humidity on the sensors and measurement results while maintaining their low cost? In this work, an experimental study is conducted to analyze the suitability of low-cost sensors for measuring submicron aerosol particles. A comparison of the measuring capability of two different low-cost sensor types and commercial measuring devices is carried out. The influence of the humidity on the measuring capability was investigated by varying the relative humidity of the air flow and the use of a heating stage for drying. The related measurement problems with low-cost sensors led to the development and investigation of a drying process for potential room monitoring.

2. Experimental Setup

2.1. Measurement Devices

The experimental investigation was performed with four different measurement devices. Table 1 summarizes the relevant specifications of measurement devices used in this study to detect particle mass and number concentrations in aerosols. They differ in the measurement method, measured particle size range, and cost.

The Scanning Mobility Particle Sizer (SMPS, TSI Model No. 3934) from TSI GmbH is a commonly used laboratory-scale device for particles in the nanometer size range. It classifies the particles based on their electric potential and then determines the number of particles in individual fractions by spectrometry [38]. For the investigations with the low-cost sensors, two different models were selected: the SDS011 from NovaFitness and the HPMA compact from Honeywell. Their photometric measuring method operates via transmission effects, which results in a wider detectable particle-size range than with the SMPS. There are already a number of studies with the mentioned low-cost sensors [39–44], where the comparison to different laboratory measuring devices (Optical Particle Counter, SMPS, etc.) showed that the PM_{2.5} values are comparable [39,41,43]. As soon as the range allowed by the manufacturer for the relative humidity is exceeded, the measured values are detected incorrectly [41,44]. The low-cost sensors output their results in PM_{2.5} and PM₁₀, which correspond to the particle mass concentration of all particles up to 2.5 μm

and 10 μm , respectively. In addition, the Air Quality Guard (AQ Guard) from Palas GmbH is used, which promises to detect a wide range of particle sizes, including their mass and number concentration, using the photometric measuring method [14]. Considering this, it is referred to as a mid-cost device.

Table 1. Specifications of the used measuring devices.

Model	SMPS 3934	AQ Guard	SDS011	HPMA Compact
Company	TSI GmbH	Palas GmbH	NovaFitness	Honeywell
Measuring device	Lab-scale devices		Low-cost sensors	
Measurement range μm	0.014 to 1	0.175 to 20	0.3 to 10	N/A
Measurement method	Spectrometer	Spectrometer	Photometer	Photometer
Mass conc. $\mu\text{g}\cdot\text{m}^{-3}$	-	$\text{max. } 2 \cdot 10^4$	$\text{max. } 10^3$	$\text{max. } 10^3$
Number conc. cm^{-3}	$2 \cdot 10^6$	$\text{max. } 2 \cdot 10^4$	-	-
Flow rate $\text{l} \cdot \text{min}^{-1}$	0.3	1.0	0.3	0.1
Costs €	>50,000	>5000	<50	<50

2.2. Test Setup

For the experimental investigations of the suitability of low-cost sensors for the measurement of submicron aerosol droplets and particles, the test rig shown in Figure 1 was used.

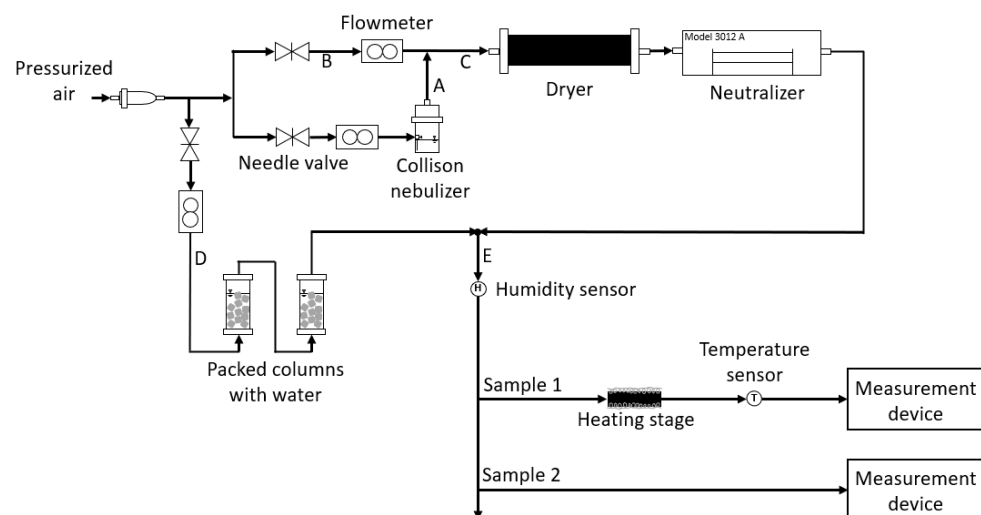


Figure 1. Test setup for the experimental investigations of aerosols.

The test aerosol is generated with a self-constructed Collision nebulizer using pressurized air (particle-free due to filtration with a HEPA filter) [45]. The mixing ratio between the stream after the nebulizer (A) and the particle-free air (B) determines the resulting particle concentration (C). After that, the aerosol is passed through a diffusion dryer with silica gel and an aerosol neutralizer (TSI Model 3012A) to obtain a bipolar equilibrium charge distribution [46,47].

An optional second stream of the pressurized air (D) is passed through two packing columns with water to increase the relative humidity. The mixing ratio between this stream

and the preconditioned aerosol determines the humidity and volume flow of the final aerosol (E). The conditioned aerosol is then led into the test section, where two samples can be measured simultaneously. Various measuring devices can be installed to detect the temperature, the particle size distribution and the particle mass concentration. In addition, a self-developed heating stage and humidity monitor can be placed in front of the sensors for further humidity control. To record the operating parameters, flowmeters from TSI (4000 Series) and sensors from Ahlborn (FHA646-E7C) were used for the aerosol temperature and humidity.

The aerosol conditioning in terms of humidification is realized with two unsorted cylindrical packing columns made of PMMA (polymethyl methacrylate) tubes, each with a length of 300 mm and a diameter of 80 mm. The column is filled with approx. 1 L distilled water. A packing of irregular plastic particles with a mean size of 2 cm is added to the column, which increases the surface of the phase boundary and enhances the mass transfer. The airflow is humidified by passing through the deionized water. In terms of drying the aerosol, a heating stage is designed and constructed. It is based on a 200 mm long copper tube with an outer diameter of 10 mm and a wall thickness of 1 mm. The material is characterized by its very high thermal conductivity properties and its good availability, which makes it suitable for this heat transfer application. At each end of the tube, there are tapers to the 6 mm outer diameter to fit the heating section into the test rig. The heating resistance wire made of copper–nickel alloy is wound on the tube. The heating wire is connected to a laboratory power supply by means of two cables, whereby voltages up to 25 V can be set. The correlation between the heating voltage and the specific electrical energy is shown in Figure 2.

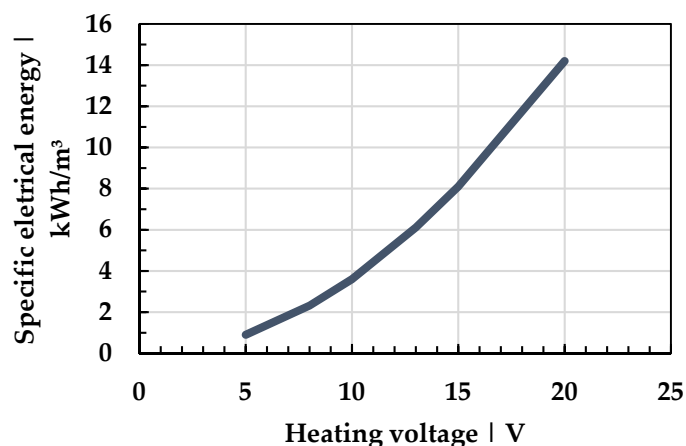


Figure 2. Specific electrical energy depending on the voltage of the heating stage at a volume flow of $0.17 \text{ L}\cdot\text{min}^{-1}$.

For low specific energy inputs under $3.5 \text{ kWh}\cdot\text{m}^{-3}$, the temperature is nearly room temperature. In this case, the natural convection counteracts the heating process. For greater energy inputs, the temperature increases in an almost linear correlation. The explicit influence of the heating just starts at $6 \text{ kWh}\cdot\text{m}^{-3}$.

2.3. Submicron Aerosol Particles

In this study, a defined aerosol of sodium chloride (NaCl) is used for the investigation of the particle mass concentration. NaCl is characterized by its environmentally and user-friendly chemical properties and easy handling. For this reason, it is a commonly used material for aerosol investigations [48–56].

The aerosol mass concentration is regulated by the sodium chloride concentration of the water solution in the Collison nebulizer. The mixing ratio (B:A in Figure 1) is set at a constant of 6:1, resulting in a total volume flow of $30 \text{ L}\cdot\text{min}^{-1}$. The particle size distribution (PSD) of the generated aerosol is measured with the SMPS at position Sample 1. For

the lowest-used NaCl concentration ($0.25 \text{ g}\cdot\text{L}^{-1}$), the PSD is shown in Figure 3, with an image from the scanning electron microscope (SEM, Model SU8000, Hitachi High-Tech Corporation, Krefeld, Germany). The sample was taken by the Nanometer Aerosol Sampler (Model 3089, TSI GmbH, Aachen, Germany).

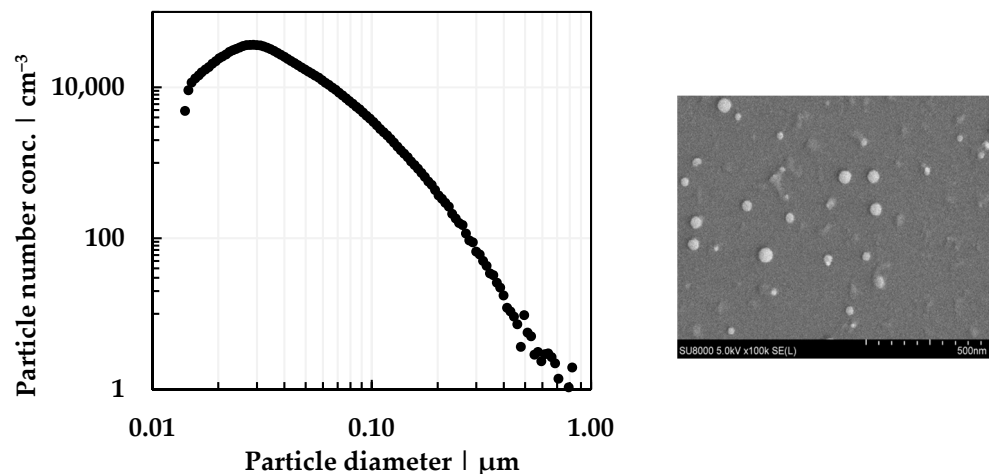


Figure 3. Particle size distribution and SEM image of sodium chloride particles used in experiments, nebulizer concentration $0.25 \text{ g}\cdot\text{L}^{-1}$, humidity of the aerosol at 15%.

The measured particle size range is between 14 and 800 nm, and the modal diameter is about 30 nm. The SEM image in Figure 3 demonstrates the particle shape, which can be assumed to be spherical. The course of the PSD stays the same for different concentrations of sodium chloride, only the total particle number changes [45]. The smallest particle size corresponds to the detection limit of the measuring device. However, the distribution curve indicates that smaller nanoparticles are also in the system. The broad size distribution of NaCl particles is suitable for all size ranges of the sensors in Table 1 and thus enables investigations under the same conditions.

3. Results and Discussion

3.1. Influence of Different Aerosol Particle Concentrations on the Measurement Capability and Accuracy of the Low-Cost Sensors

To investigate the measurement capability of the different low-cost sensors with the previously shown test setup (cf. Section 2.2), various concentrations of NaCl (0.25 , 0.5 , 0.75 , and $1.0 \text{ g}\cdot\text{L}^{-1}$) in solution were used for the Collison nebulizer. The mixing ratio of B:A is set to 6:1 (particle-free air: NaCl aerosol), with a total volume flow of $30 \text{ L}\cdot\text{min}^{-1}$. At this flow condition, the relative aerosol humidity is reduced in the diffusion dryer to a constant level below 15% for all measurements at the sample stage. For the following investigations, the temperature is also constant at $25 \text{ }^\circ\text{C}$. During the measurement, the low-cost sensor is installed at the first sample position, and the Palas AQ Guard is placed at position two.

The particle mass concentrations (PM_{2.5}) are measured with the low-cost sensors: SDS011 and HPMA compact. In Figure 4, the results for NaCl aerosols produced from NaCl solutions of four different concentrations up to $1.0 \text{ g}\cdot\text{L}^{-1}$ in the disperser are shown. Each data point results from repeated measurements, with three samples from each sensor and multiple measurements of each (a total of at least nine). The PM₁₀ values are not plotted as they are identical to the PM_{2.5} values. This observation is consistent with the measurements of the PSD (Figure 3), which does not contain any particles larger than $2.5 \text{ }\mu\text{m}$.

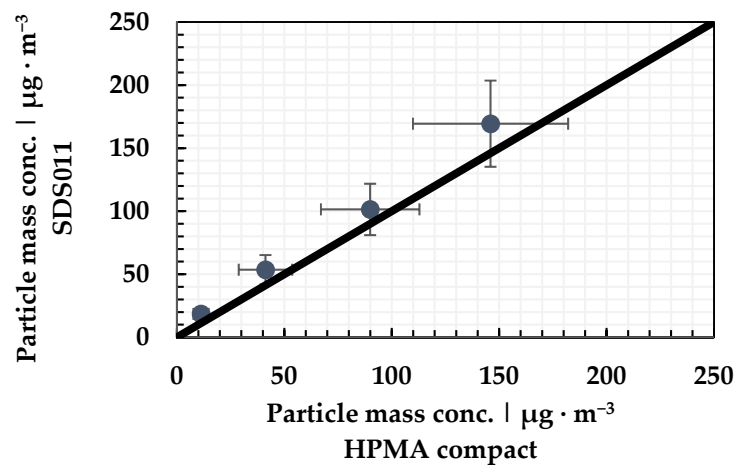


Figure 4. Comparison of PM_{2.5} measurements between SDS011 and HPMA compact at identical operating conditions.

The measurement performance of the low-cost sensors is comparable. The SDS011 sensor just shows a slightly higher detection capacity at higher aerosol concentrations. The standard deviation increases with higher particle concentrations; however, a decrease in the coefficient of variation (CV) can be observed. At the highest particle concentration, it is approximately 20% for both low-cost sensors. This is due to the difference between the individual models of one sensor type and cannot be attributed to fluctuating aerosol generation. This is confirmed by the comparison to the relative deviation in the parallel measurements with the AQ Guard, which is less than 7%. This is also consistent with the PSD measurements with the SMPS (cf. Section 2.3).

In the same experiment, the aerosol is measured with the AQ Guard as well as the low-cost sensors. The resulting particle mass concentrations (PM_{2.5}) are shown in Figure 5 in comparison to the dataset of the low-cost sensors.

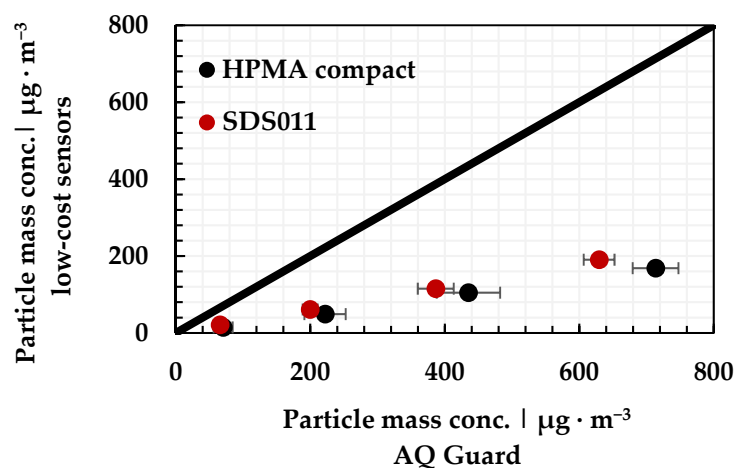


Figure 5. Comparison of PM_{2.5} measurements between AQ Guard and low-cost sensors (SDS011 and HPMA compact) at identical operating conditions.

The detected PM_{2.5} values of the AQ Guard are much higher, showing a clear deviation from the results of the low-cost sensors. This observation can initially be related to the different particle-size detection ranges of the sensors. The smallest particle size is 0.175 μm for the AQ Guard, 0.3 μm for the SDS011 and not known for the HPMA compact. Regarding the PSD of the used NaCl particle system (cf. Figure 3), the number of particles in this size range rises significantly and might explain this deviation. Besides the mass concentration, the AQ Guard detects the number-based particle concentration and its distribution. From

this, the size range can be tailored to match that of the low-cost sensors. This new number distribution is then calculated for the mass concentration using the assumptions of constant density and spherical particle shape. Unfortunately, the PM values of the AQ Guard do not match those of the low-cost sensors either. The reason for the deviation cannot be clearly determined; in general, this can be attributed to the unknown system internal calibrations, as well as the limits of the optical measurement technology that are reached in this particle size range. Despite this, the results show that both low-cost sensors are suitable for the qualitative measurement of particle concentration.

3.2. Influence of Aerosol Humidity on Measurement Capability and Accuracy of the Low-Cost Sensors

This section describes the influence of humidity on the measurements of the low-cost sensors. The indoor relative humidity is usually between 40 and 60% [57]. Initially, the test aerosol must be adequately conditioned, and for this purpose particle-free air is led through one or two columns (series) and then mixed with the dry NaCl aerosol (cf. Section 2.3). The mixing ratio of these two flows (C:D) determines the resulting humidity. Figure 6 shows the possible relative humidity for both configurations at different flow rates.

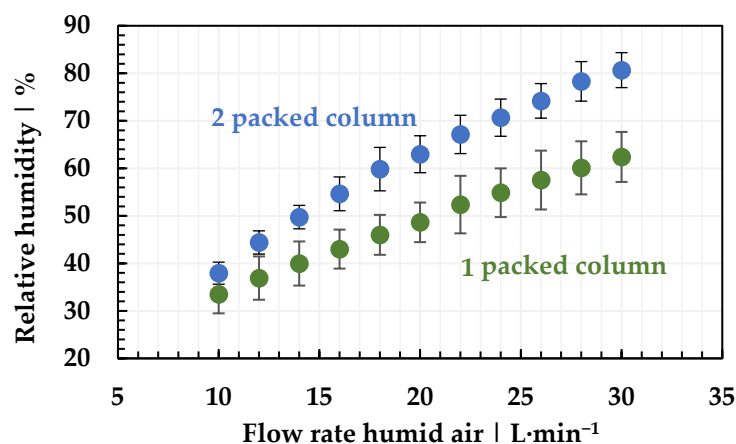


Figure 6. Relative humidity depending on the flow rate of the humid air (D), at a constant NaCl (C) aerosol flow of $4 \text{ L}\cdot\text{min}^{-1}$, using a single column or two in series.

An increase in the saturated air-flow rate leads to an increase in the relative humidity of the total air flow, while the air-flow rate of the test aerosol is constant at $4 \text{ L}\cdot\text{min}^{-1}$. Using one column, a maximum humidity of approx. 60% can be achieved; with two columns, a maximum of approx. 80% is possible. The divergence of the results is caused by the uneven mass transfer in a random packing. The study of the influence of humidity on the measuring capability of PM is carried out with the low-cost sensor SDS011. Figure 7 shows the resulting PM concentrations of the SDS011 sensor for the particle-free air flow and for the NaCl aerosol, depending on the relative humidity.

The results for the particle-free air clearly show that the humidity has no impact on the measurement of PM values. At a constant volume flow with varying humidity, no particles are detected. Consequently, condensation on the detector or in the measuring volume can be excluded as well. Under identical conditions, the results with the conditioned NaCl aerosol show a correlation between the two parameters, and the PM values increase with increasing humidity (cf. Figure 7). Up to 60% humidity, the correlation is approximately linear, while for higher humidity levels the detected PM rises significantly. Values at 70% are about four times higher than the values at 40%. The reason for this increase in the PM values is the hygroscopic growth of the particles in humid air [58,59]. Initially, the adsorption of water-vapor molecules takes place until the maximum capacity (max. adsorption capacity of the salt) is reached. Then, water-vapor condensation and particle dissolution occur (solubility point), which leads to a growth process, and the solid particle

becomes a droplet [60]. With the change in size, the optical properties of the particles also change—for example, their interaction with light [61].

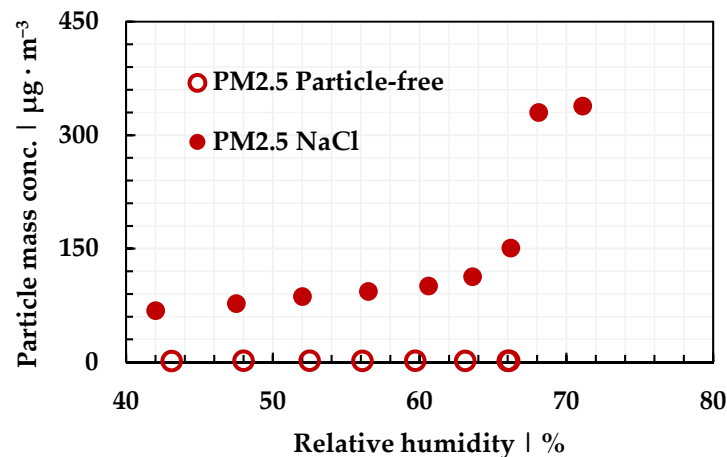


Figure 7. PM2.5 values for particle-free air depending on the relative humidity measured with the low-cost sensor SDS011, nebulizer concentration $0.25 \text{ g}\cdot\text{L}^{-1}$.

3.3. Influence of Aerosol Heating on Measurement Capability of Low-Cost Sensors under Indoor Conditions

Due to the strong influence of air humidity on particle size, aerosol measurements with low-cost sensors must take place under constant conditions. Therefore, it is necessary to control the relative humidity for indoor aerosol monitoring and keep it at a low level. This can be achieved by aerosol heating in the previously described low-cost copper heating construction (cf. Section 2.2). The relation between the heating voltage and the specific electrical energy has already been explored (cf. Figure 2).

The SDS011 low-cost sensor was combined with a heating stage (cf. Figure 1) to investigate its influence on aerosol measurements. For this purpose, continuous measurement is carried out with this low-cost unit. The NaCl aerosol (nebulizer concentration at $0.25 \text{ g}\cdot\text{L}^{-1}$) is preconditioned to approx. 70% humidity by two packed columns (cf. Section 3.2). After the PM value becomes stationary, the heating stage is turned on and operates for a period of 5 min at one energy input (up to $14 \text{ kWh}/\text{m}^3$). Figure 8 shows the PM results for the operating points at approximately 6, 8 and $10 \text{ kWh}/\text{m}^3$. In addition, the heating time is marked (gray area).

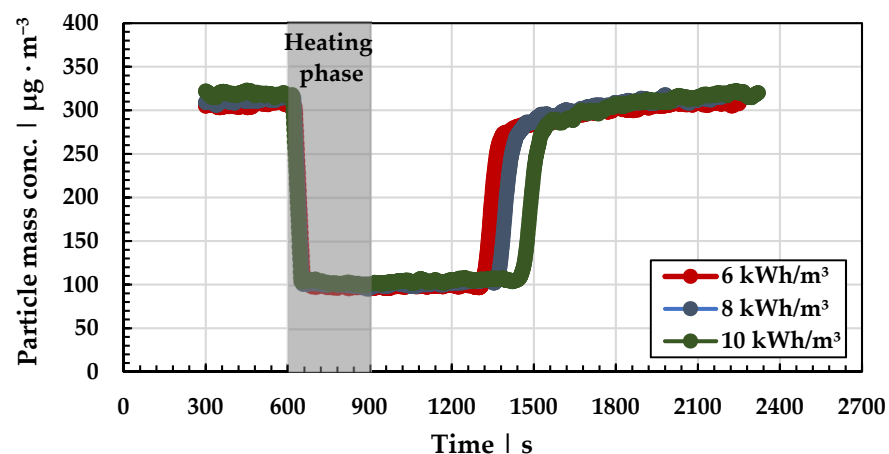


Figure 8. PM2.5 values measured over time with the SDS011 low-cost sensor at a relative humidity of 70% and a specific electrical energy of 6, 8 and $10 \text{ kWh}/\text{m}^3$.

The recorded PM_{2.5} value before the heating corresponds to the data from Section 3.2. A significant abrupt drop in PM_{2.5} can be observed after starting the heating process, after which the value remains at a constant level. Further heating no longer influences the particle concentration. After the heating element has been switched off, the PM value is still the same as previously and remains constant for a period of time. Subsequently, the PM_{2.5} value rises again and rapidly returns to its initial value. The time interval between the heating end and PM recovery is hereafter referred to as residence time. Studies on the lower and higher power inputs show the similar behavior of the particle concentrations. The PM_{2.5} value measured during the heating phase and afterwards is the same in all experiments and remains at approx. $100 \mu\text{g}\cdot\text{m}^{-3}$. The curves in Figure 8 only differ in the time until the PM drops after the start of the heating process and the duration of the residence time. For low-energy inputs, the influence of the heating appears to be time-delayed, while for higher inputs it occurs nearly instantly. The residence time increases with increasing specific electrical energy.

The results show that the heating stage fulfills its purpose of reducing the effect of humidity on particle size and therefore improves the measurement of aerosol-particle mass concentration. It is surprising that the PM level instantaneously drops and remains at the same value regardless of heating time. It is probable that a critical stable humidity is reached inside the heating stage, which leads to the abrupt changes in the PM values. The increasing residence time for higher specific electric energy is presumably caused by residual heat that is still being emitted into the aerosol even after the heating section has been switched off. The greater the input energy, the longer this effect lasts. The observed effects must be further investigated and the influence of the initial humidity and the volume flow on the constant PM level and the residence time must be clarified. Based on the current results, the heating stage seems applicable for both low and high power consumption. In this context, an energy-optimized indoor-air-quality measurement guide can be developed that coordinates measurements and heating intervals.

4. Conclusions

In this work, the measurement capability of low-cost sensors for particle mass concentration in aerosols in the submicron range was investigated and compared to SMPS and AQ Guard sensors. Furthermore, the influence of humidity and the drying process were determined as variables. It was shown that the measurement performance of the two different low-cost sensors (SDS011 and HPMA compact) is comparable. However, in comparison to the laboratory devices, different PM_{2.5} values were obtained by low-cost sensors, which can be explained by different measuring ranges and methods. The impact of an increase in the relative humidity to over 65%, using water-soluble sodium-chloride particles, on the measurement behavior of the sensors had a negative effect on PM measurements due to hygroscopic droplet growth. A simple electrical heating stage, which can be installed in front of the low-cost sensor, improved the measurement of the PM values significantly. Despite some disadvantages of the low-cost sensors, they have the potential to detect indoor aerosol spreading. Based on these data, hygiene concepts for air-quality improvement and infection prevention can be developed.

Author Contributions: Conceptualization, D.S., M.K. and S.P.; methodology, D.S., M.K. and S.P.; software, D.S. and S.P.; validation, D.S. and S.P.; formal analysis, D.S. and S.P.; investigation, D.S. and S.P.; resources, D.S. and S.P.; data curation, D.S. and S.P.; writing—original draft preparation, D.S. and S.P.; writing—review and editing, D.S.; visualization, D.S. and S.P.; supervision, S.A.; project administration, D.S.; funding acquisition, M.K. and S.A.; All authors have read and agreed to the published version of the manuscript.

Funding: This research was funded by the VolkswagenStiftung (99604).

Informed Consent Statement: Not applicable.

Data Availability Statement: Not applicable.

Acknowledgments: This work was performed within the project “Development of a low-cost sensor for aerosol spread monitoring”. The project (99604) was funded via the VolkswagenStiftung “Corona Crisis and Beyond—Perspectives for Science, Scholarship and Society”.

Conflicts of Interest: The authors declare no conflict of interest. The funders had no role in the design of the study; in the collection, analyses, or interpretation of data; in the writing of the manuscript; or in the decision to publish the results.

References

- Jin, Y.-H.; Cai, L.; Cheng, Z.-S.; Cheng, H.; Deng, T.; Fan, Y.-P.; Fang, C.; Huang, D.; Huang, L.-Q.; Huang, Q.; et al. A rapid advice guideline for the diagnosis and treatment of 2019 novel coronavirus (2019-nCoV) infected pneumonia (standard version). *Mil. Med. Res.* **2020**, *7*, 4. [[CrossRef](#)] [[PubMed](#)]
- Asadi, S.; Bouvier, N.; Wexler, A.S.; Ristenpart, W.D. The coronavirus pandemic and aerosols: Does COVID-19 transmit via expiratory particles? *Aerosol Sci. Technol.* **2020**, *54*, 635–638. [[CrossRef](#)]
- Stadnytskyi, V.; Anfinrud, P.; Bax, A. Breathing, speaking, coughing or sneezing: What drives transmission of SARS-CoV-2? *J. Intern. Med.* **2021**, *290*, 1010–1027. [[CrossRef](#)] [[PubMed](#)]
- Noorimotlagh, Z.; Jaafarzadeh, N.; Martínez, S.S.; Mirzaee, S.A. A systematic review of possible airborne transmission of the COVID-19 virus (SARS-CoV-2) in the indoor air environment. *Environ. Res.* **2020**, *193*, 110612. [[CrossRef](#)]
- Rowe, B.; Canosa, A.; Drouffe, J.; Mitchell, J. Simple quantitative assessment of the outdoor versus indoor airborne transmission of viruses and COVID-19. *Environ. Res.* **2021**, *198*, 111189. [[CrossRef](#)]
- Chao, C.Y.H.; Wan, M.P.; Morawska, L.; Johnson, G.R.; Ristovski, Z.D.; Hargreaves, M.; Mengersen, K.; Corbett, S.; Li, Y.; Xie, X.; et al. Characterization of expiration air jets and droplet size distributions immediately at the mouth opening. *J. Aerosol Sci.* **2009**, *40*, 122–133. [[CrossRef](#)]
- Stiti, M.; Castanet, G.; Corber, A.; Alden, M.; Berrocal, E. Transition from saliva droplets to solid aerosols in the context of COVID-19 spreading. *Environ. Res.* **2022**, *204*, 112072. [[CrossRef](#)] [[PubMed](#)]
- Lieber, C.; Melekidis, S.; Koch, R.; Bauer, H.-J. Insights into the evaporation characteristics of saliva droplets and aerosols: Levitation experiments and numerical modeling. *J. Aerosol Sci.* **2021**, *154*, 105760. [[CrossRef](#)]
- Holmgren, H.; Ljungström, E.; Almstrand, A.-C.; Bake, B.; Olin, A.-C. Size distribution of exhaled particles in the range from 0.01 to 2.0 μm. *J. Aerosol Sci.* **2010**, *41*, 439–446. [[CrossRef](#)]
- Holmgren, H.; Bake, B.; Olin, A.-C.; Ljungström, E. Relation Between Humidity and Size of Exhaled Particles. *J. Aerosol Med. Pulm. Drug Deliv.* **2011**, *24*, 253–260. [[CrossRef](#)]
- Antonyuk, S.; Kerner, M.; Misiulia, D. Untersuchung einer Testabluftanlage zur Reduzierung der Aerosolausbreitung in Schulräumen. *FS Filtr. Sep.* **2021**, *3*, 3–8.
- Ciužas, D.; Prasauskas, T.; Krugly, E.; Sidaraviciute, R.; Jurelionis, A.; Seduikyte, L.; Kauneliene, V.; Wierzbicka, A.; Martuzevicius, D. Characterization of indoor aerosol temporal variations for the real-time management of indoor air quality. *Atmos. Environ.* **2015**, *118*, 107–117. [[CrossRef](#)]
- Tu, K.-W.; Knutson, E.O. Indoor Outdoor Aerosol Measurements for Two Residential Buildings in New Jersey. *Aerosol Sci. Technol.* **1988**, *9*, 71–82. [[CrossRef](#)]
- Oberst, M.; Klar, T.; Heinrich, A. The effect of mobile air filter systems on aerosol concentrations in large volume scenarios against the background of the risk of infection of COVID-19. Can classroom teaching be resumed? *Zentralblatt Arbeitsmedizin Arbeitsschutz Ergon.* **2021**, *71*, 205–212. [[CrossRef](#)]
- Zimmerman, N. Tutorial: Guidelines for implementing low-cost sensor networks for aerosol monitoring. *J. Aerosol Sci.* **2021**, *159*, 105872. [[CrossRef](#)]
- Thompson, J.E. Crowd-sourced air quality studies: A review of the literature & portable sensors. *Trends Environ. Anal. Chem.* **2016**, *11*, 23–34. [[CrossRef](#)]
- Clements, A.; Griswold, W.; Ahijit, R.; Johnston, J.; Herting, M.; Thorson, J.; Collier-Oxandale, A.; Hannigan, M. Low-Cost Air Quality Monitoring Tools: From Research to Practice (A Workshop Summary). *Sensors* **2017**, *17*, 2478. [[CrossRef](#)] [[PubMed](#)]
- Kumar, P.; Martani, C.; Morawska, L.; Norford, L.; Choudhary, R.; Bell, M.; Leach, M. Indoor air quality and energy management through real-time sensing in commercial buildings. *Energy Build.* **2016**, *111*, 145–153. [[CrossRef](#)]
- Hegde, S.; Min, K.T.; Moore, J.; Lundrigan, P.; Patwari, N.; Collingwood, S.; Balch, A.; Kelly, K.E. Indoor Household Particulate Matter Measurements Using a Network of Low-cost Sensors. *Aerosol Air Qual. Res.* **2020**, *20*, 381–394. [[CrossRef](#)]
- Weekly, K.; Rim, D.; Zhang, L.; Bayen, A.M.; Nazaroff, W.W.; Spanos, C.J. Low-cost coarse airborne particulate matter sensing for indoor occupancy detection. In Proceedings of the 2013 IEEE International Conference on Automation Science and Engineering (CASE), Madison, WI, USA, 17–20 August 2013; pp. 89–94. [[CrossRef](#)]
- Nguyen, P.D.M.; Martinussen, N.; Mallach, G.; Ebrahimi, G.; Jones, K.; Zimmerman, N.; Henderson, S.B. Using Low-Cost Sensors to Assess Fine Particulate Matter Infiltration (PM_{2.5}) during a Wildfire Smoke Episode at a Large Inpatient Healthcare Facility. *Int. J. Environ. Res. Public Health* **2021**, *18*, 9811. [[CrossRef](#)]
- Alonso, M.J.; Moazami, T.; Liu, P.; Jørgensen, R.; Mathisen, H. Assessing the indoor air quality and their predictor variable in 21 home offices during the Covid-19 pandemic in Norway. *Build. Environ.* **2022**, *225*, 109580. [[CrossRef](#)] [[PubMed](#)]

23. Zanni, S.; Motta, G.; Mura, M.; Longo, M.; Caiulo, D. The Challenge of Indoor Air Quality Management: A Case Study in the Hospitality Industry at the Time of the Pandemic. *Atmosphere* **2021**, *12*, 880. [[CrossRef](#)]
24. Rai, A.C.; Kumar, P.; Pilla, F.; Skouloudis, A.N.; Di Sabatino, S.; Ratti, C.; Yasar, A.-U.; Rickerby, D. End-user perspective of low-cost sensors for outdoor air pollution monitoring. *Sci. Total Environ.* **2017**, *607–608*, 691–705. [[CrossRef](#)] [[PubMed](#)]
25. Karagulian, F.; Barbieri, M.; Kotsev, A.; Spinelle, L.; Gerboles, M.; Lagler, F.; Redon, N.; Crunaire, S.; Borowiak, A. Review of the Performance of Low-Cost Sensors for Air Quality Monitoring. *Atmosphere* **2019**, *10*, 506. [[CrossRef](#)]
26. Liu, X.; Jayaratne, R.; Thai, P.; Kuhn, T.; Zing, I.; Christensen, B.; Lamont, R.; Dunbabin, M.; Zhu, S.; Gao, J.; et al. Low-cost sensors as an alternative for long-term air quality monitoring. *Environ. Res.* **2020**, *185*, 109438. [[CrossRef](#)]
27. Wang, S.; Ma, Y.; Wang, Z.; Wang, L.; Chi, X.; Ding, A.; Yao, M.; Li, Y.; Li, Q.; Wu, M.; et al. Mobile monitoring of urban air quality at high spatial resolution by low-cost sensors: Impacts of COVID-19 pandemic lockdown. *Atmos. Chem. Phys.* **2021**, *21*, 7199–7215. [[CrossRef](#)]
28. Danek, T.; Zareba, M. The Use of Public Data from Low-Cost Sensors for the Geospatial Analysis of Air Pollution from Solid Fuel Heating during the COVID-19 Pandemic Spring Period in Krakow, Poland. *Sensors* **2021**, *21*, 5208. [[CrossRef](#)] [[PubMed](#)]
29. Bujňák, M.; Pirmík, R.; Kuchár, P.; Rástočný, K. Assessing the Risk of Spreading COVID-19 in the Room Utilizing Low-Cost Monitoring System. *Appl. Syst. Innov.* **2023**, *6*, 40. [[CrossRef](#)]
30. Giordano, M.R.; Malings, C.; Pandis, S.N.; Presto, A.A.; McNeill, V.; Westervelt, D.M.; Beekmann, M.; Subramanian, R. From low-cost sensors to high-quality data: A summary of challenges and best practices for effectively calibrating low-cost particulate matter mass sensors. *J. Aerosol Sci.* **2021**, *158*, 105833. [[CrossRef](#)]
31. Zheng, T.; Bergin, M.H.; Johnson, K.K.; Tripathi, S.N.; Shirodkar, S.; Landis, M.S.; Sutaria, R.; Carlson, D.E. Field evaluation of low-cost particulate matter sensors in high- and low-concentration environments. *Atmos. Meas. Tech.* **2018**, *11*, 4823–4846. [[CrossRef](#)]
32. Sayahi, T.; Butterfield, A.; Kelly, K.E. Long-term field evaluation of the Plantower PMS low-cost particulate matter sensors. *Environ. Pollut.* **2019**, *245*, 932–940. [[CrossRef](#)] [[PubMed](#)]
33. Yoon, S.-C.; Kim, J. Influences of relative humidity on aerosol optical properties and aerosol radiative forcing during ACE-Asia. *Atmos. Environ.* **2006**, *40*, 4328–4338. [[CrossRef](#)]
34. Zieger, P.; Fierz-Schmidhauser, R.; Weingartner, E.; Baltensperger, U. Effects of relative humidity on aerosol light scattering: Results from different European sites. *Atmos. Chem. Phys.* **2013**, *13*, 10609–10631. [[CrossRef](#)]
35. Randriamiarisoa, H.; Chazette, P.; Couvert, P.; Sanak, J.; Mégie, G. Relative humidity impact on aerosol parameters in a Paris suburban area. *Atmos. Chem. Phys.* **2006**, *6*, 1389–1407. [[CrossRef](#)]
36. Young, P.M.; Sung, A.; Traini, D.; Kwok, P.; Chiou, H.; Chan, H.-K. Influence of Humidity on the Electrostatic Charge and Aerosol Performance of Dry Powder Inhaler Carrier based Systems. *Pharm. Res.* **2007**, *24*, 963–970. [[CrossRef](#)]
37. Li, J.; Xu, W.; Li, Z.; Duan, M.; Ouyang, B.; Zhou, S.; Lei, L.; He, Y.; Sun, J.; Wang, Z.; et al. Real-time characterization of aerosol particle composition, sources and influences of increased ventilation and humidity in an office. *Indoor Air* **2021**, *31*, 1364–1376. [[CrossRef](#)]
38. Stieß, M. *Mechanische Verfahrenstechnik—Partikeltechnologie 1*, 3rd ed.; Springer: Berlin/Heidelberg, Germany, 2009. [[CrossRef](#)]
39. Afroz, M.R.; Guo, X.; Cheng, C.-W.; Delorme, A.; Duruisseau-Kuntz, R.; Zhao, R. Investigation of indoor air quality in university residences using low-cost sensors. *Environ. Sci. Atmos.* **2023**, *3*, 347–362. [[CrossRef](#)]
40. Wardoyo, A.Y.P.; Dharmawan, H.A.; Nurhuda, M.; Adi, E.T.P. Optimization of PM_{2.5} Measurement System Using NOVA SDS011 Sensor. *J. Phys. Conf. Ser.* **2020**, *1428*, 012053. [[CrossRef](#)]
41. Budde, M.; Schwarz, A.D.; Müller, T.; Laquai, B.; Streibl, N.; Schindler, G.; Köpke, M.; Riedel, T.; Dittler, A.; Beigl, M. Potential and Limitations of the Low-Cost SDS011 Particle Sensor for Monitoring Urban Air Quality. *ProScience* **2018**, *5*, 12. [[CrossRef](#)]
42. Horender, S.; Tancev, G.; Auderset, K.; Vasilatou, K. Traceable PM_{2.5} and PM₁₀ Calibration of Low-Cost Sensors with Ambient-like Aerosols Generated in the Laboratory. *Appl. Sci.* **2021**, *11*, 9014. [[CrossRef](#)]
43. Jayaratne, R.; Liu, X.; Ahn, K.-H.; Asumadu-Sakyi, A.; Fisher, G.; Gao, J.; Mabon, A.; Mazaheri, M.; Mullins, B.; Nyarku, M.; et al. Low-cost PM_{2.5} Sensors: An Assessment of Their Suitability for Various Applications. *Aerosol Air Qual. Res.* **2020**, *20*, 520–532. [[CrossRef](#)]
44. Tagle, M.; Rojas, F.; Reyes, F.; Vásquez, Y.; Hallgren, F.; Lindén, J.; Kolev, D.; Watne, K.; Oyola, P. Field performance of a low-cost sensor in the monitoring of particulate matter in Santiago, Chile. *Environ. Monit. Assess.* **2020**, *192*, 171. [[CrossRef](#)] [[PubMed](#)]
45. Kerner, M. *Abscheidung Submikroner Aerosolpartikeln in Elektrostatisch Ausgerüsteten Vliesstoffen—Experimentelle und Numerische Untersuchungen*; Dissertation, Schriftreihe des Lehrstuhls für Mechanische Verfahrenstechnik der TU Kaiserslautern; Technische Universität Kaiserslautern: Kaiserslautern, Germany, 2022; Volume 27, ISBN 978-3-95974-172-9.
46. Kerner, M.; Schmidt, K.; Schumacher, S.; Asbach, C.; Antonyuk, S. Electret Filters—From the Influence of Discharging Methods to Optimization Potential. *Atmosphere* **2021**, *12*, 65. [[CrossRef](#)]
47. Wiedensohler, A. An approximation of the bipolar charge distribution for particles in the submicron size range. *J. Aerosol Sci.* **1988**, *19*, 387–389. [[CrossRef](#)]
48. Cai, C.; Floyd, E.L.; Aithinne, K.A.; Oni, T. Is the Current N95 Respirator Filtration Efficiency Test Sufficient for Evaluating Protection Against Submicrometer Particles Containing SARS-CoV-2? *medRxiv* **2020**. [[CrossRef](#)]
49. Blanchard, J.D.; Willeke, K. Total deposition of ultrafine sodium chloride particles in human lungs. *J. Appl. Physiol.* **1984**, *57*, 1850–1856. [[CrossRef](#)]

50. Weis, D.D.; Ewing, G.E. Water content and morphology of sodium chloride aerosol particles. *J. Geophys. Res. Atmos.* **1999**, *104*, 21275–21285. [[CrossRef](#)]
51. Wake, D.; Bowry, A.; Crook, B.; Brown, R. Performance of respiratory filters and surgical masks against bacterial aerosols. *J. Aerosol Sci.* **1997**, *28*, 1311–1329. [[CrossRef](#)]
52. Rengasamy, S.; Zhuang, Z.; Niezgodá, G.; Walbert, G.; Lawrence, R.; Boutin, B.; Hudnall, J.; Monaghan, W.P.; Bergman, M.; Miller, C.; et al. A comparison of total inward leakage measured using sodium chloride (NaCl) and corn oil aerosol methods for air-purifying respirators. *J. Occup. Environ. Hyg.* **2018**, *15*, 616–627. [[CrossRef](#)]
53. Sickbert-Bennett, E.E.; Samet, J.M.; Clapp, P.W.; Chen, H.; Berntsen, J.; Zeman, K.L.; Tong, H.; Weber, D.J.; Bennett, W.D. Filtration Efficiency of Hospital Face Mask Alternatives Available for Use During the COVID-19 Pandemic. *JAMA Intern. Med.* **2020**, *180*, 1607–1612. [[CrossRef](#)]
54. Leung, W.W.F.; Sun, Q. Electrostatic charged nanofiber filter for filtering airborne novel coronavirus (COVID-19) and nano-aerosols. *Sep. Purif. Technol.* **2020**, *250*, 116886. [[CrossRef](#)]
55. Moitra, P.; Alafeef, M.; Dighe, K.; Ray, P.; Chang, J.; Thole, A.; Punshon-Smith, B.; Tolosa, M.; Ramamurthy, S.S.; Ge, X.; et al. Rapid and low-cost sampling for detection of airborne SARS-CoV-2 in dehumidifier condensate. *Biotechnol. Bioeng.* **2021**, *118*, 3029–3036. [[CrossRef](#)] [[PubMed](#)]
56. Sipkens, T.A.; Corbin, J.C.; Oldershaw, A.; Smallwood, G.J. Particle filtration efficiency measured using sodium chloride and polystyrene latex sphere test methods. *Sci. Data* **2022**, *9*, 756. [[CrossRef](#)] [[PubMed](#)]
57. Asbach, C.; Schumacher, S.; Bässler, M.; Spreitzler, M.; Pohl, T.; Weber, K.; Monz, C.; Bieder, S.; Schultze, T.; Todea, A.M. Anwendungsmöglichkeiten und Grenzen kostengünstiger Feinstaubsensoren. *Reinhalt. Luft* **2018**, *78*, 242–250.
58. Haryanto, H. *Einfluss der relativen Feuchte auf die Größe von Flugaschepartikeln*, Forschungszentrum Karlsruhe; Technik und Umwelt—Wissenschaftlicher Bericht FZKA 6183; Forschungszentrum Karlsruhe: Karlsruhe, Germany, 1988.
59. Li, Y.; Zhou, Y.; Sun, Z.; Gu, H.; Ma, Q.; Diao, H. Analysis of hygroscopic growth properties of soluble aerosol under severe nuclear accidents conditions. *Prog. Nucl. Energy* **2020**, *127*, 103464. [[CrossRef](#)]
60. Rovelli, G.; Miles, R.E.H.; Reid, J.P.; Clegg, S.L. Accurate Measurements of Aerosol Hygroscopic Growth over a Wide Range in Relative Humidity. *J. Phys. Chem. A* **2016**, *120*, 4376–4388. [[CrossRef](#)] [[PubMed](#)]
61. Freney, E.J.; Adachi, K.; Buseck, P.R. Internally mixed atmospheric aerosol particles: Hygroscopic growth and light scattering. *J. Geophys. Res. Atmos.* **2010**, *115*, 210. [[CrossRef](#)]

Disclaimer/Publisher’s Note: The statements, opinions and data contained in all publications are solely those of the individual author(s) and contributor(s) and not of MDPI and/or the editor(s). MDPI and/or the editor(s) disclaim responsibility for any injury to people or property resulting from any ideas, methods, instructions or products referred to in the content.